Clinical Neurophysiology 168 (2024) 43–51

Contents lists available at ScienceDirect

Clinical Neurophysiology

journal homepage: www.elsevier.com/locate/clinph

Resting-state EEG spectral and fractal features in dementia with Lewy bodies with and without visual hallucinations

Antonino Vallesi [a,b,1,*], Camillo Porcaro [a,b,c,d,1], Antonino Visalli [e,f], Davide Fasolato [a], Francesco Rossato [a], Cinzia Bussè [a], Annachiara Cagnin [a,b,*]

[a] Dipartimento di Neuroscienze, Università degli Studi di Padova, Italy
[b] Padova Neuroscience Center, Università degli Studi di Padova, Italy
[c] Institute of Cognitive Sciences and Technologies—National Research Council, Rome, Italy
[d] Centre for Human Brain Health and School of Psychology, University of Birmingham, Birmingham, United Kingdom
[e] IRCCS San Camillo Hospital, Lido di Venezia, Venice, Italy
[f] Dipartimento di Psicologia Generale, University of Padova, Italy

ARTICLE INFO

Keywords:
Visual Hallucinations
Higuchi's Fractal Dimension
Dementia with Lewy bodies
Individual Alpha Frequency
Quantitative EEG
Alzheimer disease

ABSTRACT

Objective: Complex visual hallucinations (VH) are a core feature of dementia with Lewy bodies (DLB), though they may not occur in all patients. Power spectral density (PSD) analysis of resting-state EEG (rs-EEG) shows associations between some frequency bands (e.g., theta), individual alpha frequency (IAF) and VH. However, new tools that improve early differential diagnosis and symptom-based stratification with higher sensitivity and specificity, even within the DLB population, are desirable. We aimed to assess differences in rs-EEG data between DLB patients with VH (DLB-VH+) and without VH (DLB-VH-), comparing innovative non-linear approaches with more traditional linear ones.

Methods: We retrospectively analyzed rs-EEG recordings of DLB-VH+, DLB-VH-, Alzheimer's disease patients and age-matched healthy controls. EEG was analyzed using the nonlinear Higuchi's Fractal Dimension (FD) measure, and the results were compared with those of entropy and standard linear methods based on PSD and IAF.

Results: Only the FD measure could discriminate between DLB-VH+ and DLB-VH-.

Conclusions: In conclusion, rs-EEG differences between DLB-VH+ and DLB-VH- are better characterized by FD analysis than by a more traditional power spectrum approach.

Significance: This suggests that the presence of complex VH is associated with less complex brain dynamics at rest, as reflected by the FD measure.

1. Introduction

Dementia with Lewy bodies (DLB) belongs to the broader Lewy Body disease spectrum and is the second most common type of dementia, following Alzheimer's disease. DLB is a neurodegenerative disease with progressive cognitive decline and core features including parkinsonism, fluctuating cognition with pronounced variations in sustained attention and alertness, and recurrent complex and detailed visual hallucinations (McKeith et al., 2017).

DLB is diagnosed through clinical evaluation and supportive biomarkers identifying striatal-nigral degeneration, sympathetic denervation and REM sleep behavior disorder (McKeith et al., 2017). However, challenges arise from discrepancies between frequency of clinical and pathological diagnoses, stemming from the absence of certain core features in early stages or throughout the entire disease course (Nelson et al., 2010), as well as symptom overlap and even comorbidity with Alzheimer's disease (Merdes et al., 2003).

Due to these challenges, ongoing research aims to identify neuroimaging, neurophysiological and fluid biomarkers to enhance diagnostic and prognostic accuracy (McKeith et al., 2017; Oppedal et al., 2019). This includes exploring biomarkers obtained through expensive, radiotracer-based and and sometimes not widely available PET and SPECT imaging or through invasive lumbar puncture such as detection of a-synuclein in the CSF. Hence, there is an ongoing effort to identify

* Corresponding authors at: Dipartimento di Neuroscienze, Università degli Studi di Padova, Italy.
E-mail addresses: antonino.vallesi@unipd.it (A. Vallesi), annachiara.cagnin@unipd.it (A. Cagnin).
[1] Equal contribution.

https://doi.org/10.1016/j.clinph.2024.10.004
Accepted 9 October 2024
Available online 16 October 2024

more affordable, noninvasive, and accessible neurophysiological biomarkers that could contribute to stratifying DLB based on reported symptomatology (Aoki et al., 2019; Baik et al., 2022; Onofrj et al., 2019).

Recurrent and complex visual hallucinations (VH) stand out as one of the most pathognomonic symptoms among the core features of DLB.

VH have demonstrated high specificity for DLB, particularly in the context of a differential diagnosis with Alzheimer's disease (AD) (e.g., Jicha et al., 2010; Tiraboschi et al., 2006; Yoshizawa et al., 2013). Importantly, the general cognitive status of DLB patients, as operationalized for instance with performance on the Mini-Mental State Examination (MMSE, Folstein et al., 1975) or more specific visuo-perceptual tasks, correlates negatively with the severity, frequency or duration of complex VH (e.g., Collerton et al., 2003; D'Antonio et al., 2022). VH have also been associated with poorer outcomes and increased risk of institutionalization in DLB (Holroyd et al., 2001; Ibarretxe-Bilbao et al., 2010). Therefore, VH are of high interest for clinical and translational research. Yet, not all patients diagnosed with DLB suffer from VH, and the estimated prevalence is about 60–80 % of cases (Aarsland et al., 2001; Heitz et al., 2015; McKeith et al., 2017). Moreover, in mild cognitive impairment due to Lewy bodies pathology, the frequency of VH is estimated to be much lower than in the dementia stage (Donaghy et al., 2023).

According to the hodotopic theory of hallucinations (Ffytche, 2008), tonic whole-brain network alterations predispose to the probability of experiencing VH, that then occur due to a phasic spontaneous over-recruitment of visual regions during specific hallucination experiences. Consistent with this view, the presence of VH in DLB is associated with segregation within the ventral visual network and weakening of connectivity between fronto-parietal attentional regions and the ventral visual stream (Mehraram et al., 2022; Zorzi et al., 2021), with the presence of Lewy bodies in inferior temporal cortex (Harding et al., 2002) and dysfunction of multiple neurotransmitter systems, including the cholinergic system affecting visual and attentional brain networks (Diederich et al., 2005; Onofrj et al., 2019; Tiraboschi et al., 2000).

Hallucinating and non-hallucinating DLB have been hypothesized to be two different phenotypes of the same disease, the first being driven by specific cholinergic loss and the latter being more associated with more widespread cortical pathological alterations (Ibarretxe-Bilbao et al., 2010; Mehraram et al., 2022; Perry et al., 1990). This underscores the theoretical and clinical importance of objectively distinguishing between these two subtypes of DLB conditions. Theoretically, this would allow gaining deeper insight into the neuropathological mechanisms that differentiate these conditions. Clinically, several advantages could arise from this strategy, including the potential to facilitate earlier diagnosis, tailor treatment strategies to the specific symptomatology of each subtype, and provide more accurate prognostic information.

Potential neurophysiological biomarkers for the diagnosis should be feasible and scalable to increase their translational value for clinical practice outside basic research. In particular, quantitative EEG (qEEG) has the potential to become a biomarker for DLB, to allow a discrimination of DLB from other types of dementias, primarily AD (Bonanni et al., 2016; Chatzikonstantinou et al., 2021; Roks et al., 2008), and even a discrimination between possibly different phenotypes of the same disease, like for instance DLB with and without VH (e.g., Mehraram et al., 2022). The main benefits of the use of EEG in the diagnosis of DLB are that, besides being a direct measure of neuronal electrical activity, it is a non-invasive, relatively inexpensive and widely available procedure.

Resting-state EEG studies have quite consistently shown that patients suffering from DLB are characterized by slower oscillatory activity, with a preponderance of EEG rhythms < 8 Hz, that is, in the delta and theta (or pre-alpha) frequency range in DLB when compared with healthy controls and AD patients (see Law et al., 2020, for a review), and a reduction of alpha band activity (8–12 Hz) in DLB patients when compared to healthy age-matched controls (Bonanni et al., 2008). More specifically, the presence of hallucinations has been associated with slower EEG rhythms, including a generalized increased Theta-Beta Ratio and Theta-Alpha Ratio especially in the temporal scalp region (Baik et al., 2022; Onofrj et al., 2019). As such, posterior theta activity in resting-state EEG (rs-EEG) has been proposed as a supportive biomarker for DLB diagnostic criteria (McKeith et al., 2017); on the other hand, the severity of parkinsonism was not significantly associated with these EEG indices, suggesting that the pathogenetic mechanism underlying VH might be different from that causing other core features of DLB. Consistently, in another study, Dauwan and co-workers (2019), by analyzing resting-state MEG oscillatory brain activity, found that Parkinson's disease patients with VH had significantly higher theta power and lower beta/gamma power compared to Parkinson's disease patients without hallucinations. Moreover, in patients with DLB, theta band connectivity index (calculated as the phase-lag-based regional correlation among electrode pairs) is positively associated with the frequency and severity of VH (Peraza et al., 2018), with a possible pathogenetic role of cholinergic dysfunction (Perry et al., 1999).

Nevertheless, electrophysiological processes as also reflected by EEG are generally nonstationary and nonlinear in nature (Klonowski, 2009; Stam, 2005). Moreover, brain signals do not simply represent a sustained oscillation at a specific frequency; instead, they consist of short bouts of activity that repeat intermittently, generating more intricate nonlinear dynamics within a healthy brain system (Feingold et al., 2015; Lundqvist et al., 2016). Therefore, linear methods, including the widely used Fast Fourier transform, predominantly employed for analyzing brain oscillations in both healthy and pathological conditions, may be an oversimplification, falling short in capturing the complexity (or absence thereof) inherent in EEG signals (Cole & Voytek, 2017; Jones, 2016).

Thus, in this study, we assessed differences of rs-EEG features between hallucinated and non-hallucinated DLB patients using a non-linear measure, namely, Higuchi's Fractal Dimension (FD, Higuchi, 1988), which has frequently shown greater sensitivity compared to conventional linear spectral EEG measures when assessing signal complexity in the time domain (Kesić & Spasić, 2016; Marino et al., 2019; Porcaro et al., 2022; Cottone et al., 2017; Smith et al., 2016). FD was introduced to estimate the features of irregularly shaped objects in which a similar pattern repeats itself at different scales (Mandelbrot, The Fractal Geometry of Nature, 1983. The FD method stands out from widely used linear methods due to its notable advantages in terms of speed, accuracy, and cost, not only in research but also in clinical applications (Kesić & Spasić, 2016; Porcaro et al., 2019; Fiorenzato et al., 2023). When compared to other non-linear indicators such as entropy-based algorithms, FD has lower computational costs while still warranting high accuracy (e.g., Rubega et al., 2020; Moaveninejad et al., 2024), also showing a more accurate estimation of signal FD than alternative FD algorithms (Esteller et al. 2001; Porcaro et al. 2024).

We also compared the EEG features of these two DLB sub-groups with those of patients with AD and healthy controls. The overarching goal was to test new tools that improve early diagnosis and fine-grained symptom-based stratification also within the DLB population with higher sensitivity and specificity. We hypothesized that fractal dimension analysis of rs-EEG would have better performance in characterizing hallucinating DLB patients than by more traditional power spectrum analyses.

2. Methods

2.1. Participants

Diagnosis of probable DLB was made in accordance with the revised consensus criteria for the clinical diagnosis of DLB (McKeith et al., 2017). The presence, frequency and intensity of complex VH were documented by means of the.

NeuroPsychiatric Inventory (NPI) questionnaire (Cummings, 1997). The presence of VH was defined when the NPI-VH score was 2 or higher (range 1–12) to minimize inclusion of patients with rare and non

distressing episodes that could have been induced by external triggers, as also possible in healthy conditions. The DLB-VH+ group included 36 patients with VH (24 females) with a mean age of 77.55 years (SD = 5.62 years) and a mean MMSE score of 21.08 (SD = 5.28). The DLB-VH- group included 38 patients without VH (18 females) with a mean age of 74.43 years (SD = 7.41 years) and a mean MMSE score of 24.82 (SD = 4.19).

The study also included a group of 33 AD patients (14 females) with a mean age of 71.73 years (SD = 9.67 years) and a mean MMSE score of 21.97 (SD = 5.34), diagnosed according to current criteria (McKhann et al., 2011). For the AD group, the presence of VH was an exclusion criterion.

Finally, 27 healthy controls (HC) were also recruited (9 females). HC had a mean age of 74.89 years (SD = 9.67 years) and a mean MMSE score of 29.22 (SD = 1.09).

Table 1 reports the demographic and cognitive status characteristics for all groups. The groups differed for age ($F(3,130) = 3.09$, $p = 0.029$) and MMSE ($F(3,130) = 20.3$, $p < 0.001$), which were thus controlled for in subsequent analyses, but did not significantly differ for sex ($\chi^2(3) = 7.75$, $p = 0.051$). The education level was not available for the control participants.

Major eye diseases were not present in any patient included in this study. As regard to pharmacological psychoactive treatments in the DLB group, benzodiazepine, mostly clonazepam for RBD, were used in a similar proportion of DLB-VH+ and DLB-VH- patients (25 %); quetiapine at low doses (mean dose 39.5 ± 26 mg/day) was the only antipsychotic used almost exclusively in VH+ patients (VH+ 39 %, VH- 5 %; $p < 0.001$); only 5 patients (3 VH+ and 2 VH-) were taking low dose Levo-Dopa (mean dose: VH+ 250 ± 125 mg/day, VH-225 ± 125 mg/day). Cholinesterase inhibitors drugs were used more in the VH + group than in VH- (39 % vs 5 %, $p < 0.01$) and none was on memantine. As for the AD patients, 6.6 % were on benzodiazepine, 3 % on antipsychotic and 51.5 % on cholinesterase inhibitors drugs.

This study was approved by the Bioethical Committee of Padua University-Hospital, Italy (reference number: 0038879).

2.2. EEG data acquisition

Resting-state EEG was recorded by using the Galileo NT Line system (E.B. Neuro S.p.A.) from 21 Ag electrodes that were mounted on an elastic cap according to the international 10–20 system. Of these electrodes, 19 were recording electrodes (Fp2, Fp1, Fz, F4, F3, F8, F7, Cz, C4, C3, T4, T3, Pz, P4, P3, T6, T5, O1, O2), while the reference electrode was positioned at Fpz and the ground electrode at Oz. The impedance of the electrodes was less than 5 KΩ. The EEG signals were filtered with a time constant of 0.1 sec and a low-pass filter of 70 Hz, as well as a Notch filter set at 50 Hz. The sampling frequency was 256 Hz.

During the EEG acquisition, participants were seated in a slightly reclined chair, awake, and in a relaxed state with their eyes closed. Approximately every 2–3 min, they were asked to open their eyes for a few seconds and then close them again. After 10 min of recording, the intermittent photic stimulation (IPS) was performed, which consists of delivering light stimuli at different frequencies (3 Hz, 6 Hz, 9 Hz, 12 Hz, 15 Hz, 18 Hz, 21 Hz, 24 Hz). Between each stimulation, the participants were instructed to open and close their eyes. The IPS EEG recording is not considered in the present study. No patient reported visual hallucinations during EEG acquisition.

2.3. EEG pre-processing

Offline pre-processing of the EEG signal was performed using custom MATLAB (The MathWorks Inc., Natick, Massachusetts, United States) scripts, which included functions from the EEGLAB environment (version 2021.1 Delorme and Makeig, 2004; Barbati et al., 2004; Porcaro et al., 2015).

rs-EEG data were band-pass filtered using a Hamming windowed sinc FIR filter (cut-off frequencies = 1 and 45 Hz; default settings of the pop_eegfiltnew EEGLAB plugin). Then, the FastICA algorithm (Hyvärinen and Oja, 2000) was applied for IC decomposition. An automated IC selection of brain components was performed using the classification results of the ICLabel EEGLAB plugin (Pion-Tonachini et al., 2019) and the residual variances of the best-fitting equivalent IC dipoles calculated using the DIPFIT EEGLAB plugin. Specifically, IC with a brain label probability less than 0.7 or a best-fitting equivalent dipole with a residual variance greater than or equal to 0.15 were excluded. The mean number of excluded ICs was 9.9 (SD = 3.0) for DLB-VH+, 9.3 (SD = 2.5) for DLB-VH-, 10.4 (SD = 3.2) for AD, and 11.8 (SD = 2.9) for HC. The clean_rawdata function was used to remove noisy channels (channel criterion = 0.8, flat line criterion = 5). Removed channels were interpolated using spherical splines and continuous EEG data were re-referenced to the average of all of the EEG electrodes. Then, eye-closed rs-EEG was segmented into non-overlapping epochs of 2100 ms. The TBT EEGLAB plugin was used for the automatic rejection and interpolation of channels on an epoch-by-epoch basis. Identification of bad epochs was performed on the basis of four standard EEGLAB rejection methods: extreme values, linear trend, improbability, and kurtosis. Rejection thresholds were: +/−75 μV for the identification of the extreme values; slope exceeding 75 μV (R-square limit = 0.3) for the linear trend test; 5 SD (for each channel) and 3 SD (for all channels) for both improbability and kurtosis tests. Epochs with more than one bad channel were excluded, otherwise the bad channel was interpolated in that epoch. Channels identified as bad in more than 30 % of epochs were excluded and interpolated. The mean number of bad channels was 1.1 (SD = 0.9) for DLB-VH+, 0.7 (SD = 0.8) for DLB-VH-, 1.1 (SD = 1.0) for AD, and 1.1 (SD = 1.6) for HC.

2.4. Characterization of electrophysiological neural activity at rest

We considered signal properties in the frequency domain (PSD) and time domain. The PSD is the squared modulus of the continuous Fourier transform, and it is particularly useful for studying brain oscillations on a time scale of minutes, which is typical of an individual's "stable state" (Schomer et al., 2012). As for the time domain, signal power of neuronal assemblies, as a function of frequency, displays a "power law" function (Ramon and Holmes, 2015), and the exponent of this function corresponds to its fractality. Thus, we used temporal Higuchi's fractal

Table 1
Demographic characteristics of the sample by group.

Group	N	Age (years)		Sex		MMSE		Education (years)	
		Mean	SD	F	M	Mean	SD	Mean	SD
DLB-VH+	36	77.55	5.62	24	12	21.08	5.28	6.81	3.75
DLB-VH-	38	74.43	7.41	18	20	24.82	4.19	8.58	4.14
AD	33	71.73	9.67	14	19	21.97	5.34	8.58	4.01
HC	27	74.89	9.05	9	18	29.22	1.09	n.a.	n.a.

Abbreviations
LBD-VH+, Patients with Dementia with Lewy bodies and visual hallucinations; LBD-VH-, Patients with Dementia with Lewy bodies without visual hallucinations; AD, Patients with Alzheimer's disease; HC, healthy controls; MMSE, Mini–Mental State Examination score; N, number of individuals; SD, standard deviation; n.a., not available.

dimension (FD) (Higuchi, 1988) as a signature of neural dynamics underlying brain functions.

2.5. Higuchi's fractal dimension (FD)

Higuchi's FD (Higuchi, 1988) is a non-linear measure of waveform complexity applied in the time domain. Discretized functions or signals can be analyzed as a segment of data X(1), X(2), …, X(N), where N is the total number of samples. From the starting time sequence, a new self-similar time series X_m^k can be calculated as:

$$X_m^k : x(m), x(m+k), x(m+2k), \cdots, x\left(m+int\left(\frac{N-m}{k}\right)k\right) (1).$$

for $m = 1, 2, \ldots, k$ where m is the initial time; k is the time interval, $k = 1, 2, \ldots, k_{max}$; k_{max} is a free parameter, and $int(r)$ is the integer part of the number r.

The length, $L_m(k)$, of each curve X_m^k is calculated as:

$$L_m(k) = \frac{1}{k}\left[\sum_{i=1,int\left(\frac{N-m}{k}\right)} |X(m+ik) - X(m+(i-1)k| \frac{(N-1)/k}{int\left(\frac{N-m}{k}\right)}\right] (2).$$

where N is the length of the original time series X and $\frac{(N-1)/k}{int\left(\frac{N-m}{k}\right)}$ is a normalisation factor $L_m(k)$ was averaged for all m forming the mean value of the curve length $L(k)$ for each $k = 1, \ldots, k_{max}$ as:

$$L(k) = \frac{\sum_{m=1}^{k} L_m(k)}{k} (3).$$

An array of mean values $L(k)$ was obtained and the FD was estimated as:

$$FD = \frac{\log(L(k))}{\log(1/k)} \text{ for } k = 1, 2, \ldots, k_{max} (4).$$

In practice, the original curve or signal can be divided into smaller parts, with or without overlap, known as 'windows'. Subsequently, the FD computation method should be applied to each window, with N representing the length of the window. Individual FD values can be averaged across all windows for the entire curve (or data time-series), and the mean FD value can be used as a measure of curve complexity. FD measurements are robust with respect to the choice of window length and overlapping windows (Marino et al., 2019; Porcaro et al., 2020; Porcaro et al., 2022; Smits et al., 2016). Here, for each EEG channel, we calculated FD in non-overlapping time windows of 1 sec (corresponding to 256 time points) as a good compromise between window length of the data and computational time. The choice of the free parameter k has a crucial role in FD estimation; for this reason, for each window, we estimated 127 values of FD for all the possible k values (i.e. k = 2, …, 128). The value 128 was equal to half of the samples within our 1 sec window (i.e., 128-time points are the maximum that can be chosen since the maximum k value is equal to half of the window length). For the subsequent FD analysis, we set k = 17 (Marino et al., 2019; Porcaro et al., 2022, Porcaro et al., 2020; Smits et al., 2016). The value used for the analysis of variance (ANOVA) refers to the FD estimated for each channel and averaged across all the channels afterwards.

2.6. Entropy

For comparison, we also utilized another non-linear measure of EEG complexity known as Entropy (En). Entropy has been proposed as a measure of the variability or uncertainty associated with a given random variable. It is defined as follows:

$$E = -\sum_{i=1}^{n} P_i log P_i$$

Theoretically, En attains its global maximum when {Pi}, the probability distribution function (*pdf*) of the variable being studied, is uniformly distributed, for example, Pi ≠ Pj with i ≠ j. In the case of the measured signals, the *pdf* is unknown and should be estimated (Cohen, 2015). A well-established method for estimating the pdf is the histogram method, in which the amplitude range of the signal is linearly divided into k bins such that the ratio k/N remains constant (N corresponds to the number of signal samples). The ratio k/N characterizes the average filling of the histogram. The Freedman-Diaconis rule was used to estimate the optimal number of bins (Cohen, 2015; Freedman et al., 1981). The value used for the analysis of variance (ANOVA) refers to the entropy estimated for each channel and averaged across all the channels afterwards.

2.7. EEG power spectrum

We calculated the PSD using the Welch procedure (256 ms duration, Hanning window, and 60 % overlap). For each participant, IAF was defined as the exact frequency in the α range containing the maximum power. It was calculated using an automated peak-detection algorithm (function *RestingIAF* on EEGLab) (Corcoran et al 2018). We also extracted the EEG total power in the θ (4–7 Hz), α (8–13 Hz), and β (14–30 Hz) frequency bands (IFSECN, 1974) to calculate two indices derived from PSD estimates such as θ/α and the θ/β ratio indices (Baik et al., 2022; Onofrj et al., 2019). Before the PSD estimation, the data were normalized to zero mean and unit variance (Porcaro et al 2022; Marino et al 2019). All the indices refer to the total power value.

2.8. Exploratory linear discriminant classification

We also performed an exploratory linear discriminant classification (LDC) on DLB-VH+ vs. DLB-VH-, whose details are reported in the Supplementary Materials. The test accuracy obtained was 85.7 %. Given the relatively low number of participants, the results from this analysis should be interpreted with caution.

2.9. Statistical analysis

FD, Entropy, IAF, and the θ/α and θ/β ratios were modeled using ANCOVA with the GROUP as a fixed factor (four levels: DLB-VH+, DLB-VH-, AD, HC) and MMSE and Age (in days) as covariates (ANCOVA1). To assess the robustness of the results to analytical flexibility, we also performed the same ANCOVA without the covariate Age (ANCOVA2), and an ANOVA with the GROUP factor (i.e., the same model without covariates). Since the dependent variables θ/α and θ/β violated normality assumptions, they were Log-transformed. Post-hoc analysis was performed using the Holm correction method for multiple comparisons. All the analyses described above were conducted in JAMOVI software (v2.3.26, https://www.jamovi.org/). Tables including results from all the AN(C)OVA and post-hoc tests are reported in Supplementary Information.

3. Results

3.1. Higuchi's Fractal Dimension

The results of the ANCOVA1 on FD rs-EEG measures, which included MMSE scores and age as covariates, showed significant effects for Group ($F(3,128) = 11.205$, $p < 0.001$) and MMSE ($F(1,128) = 28.657$, $p < 0.001$), but not for Age ($F(1,128) = 0.204$, $p = 0.652$). Fig. 1A shows that FD was significantly lower for DLB-VH+ compared to all the other groups (DLB-VH+ vs. DLB VH-: $t(128) = -4.785$, $p < 001$; DLB-VH+ vs. AD: $t(128) = -5.179$, $p < 001$; DLB-VH+ vs. HC: $t(128) = -2.625$, $p = 0.039$). No other comparison was significant (all ps > 0.299). Fig. 2 shows the topography of the FD-related differences between the two DLB groups (i.e., DLB-VH+ and DLB-VH- contrasted through a non-parametric *t*-test, with FDR-corrected results), and indicates how the decrease in signal complexity is widespread across the entire scalp, corroborating our decision to average across electrodes. The results were almost identical to those obtained with ANCOVA2 (Figure S1A) and very consistent with the ANOVA (Figure S2A; see also Supplementary Information).

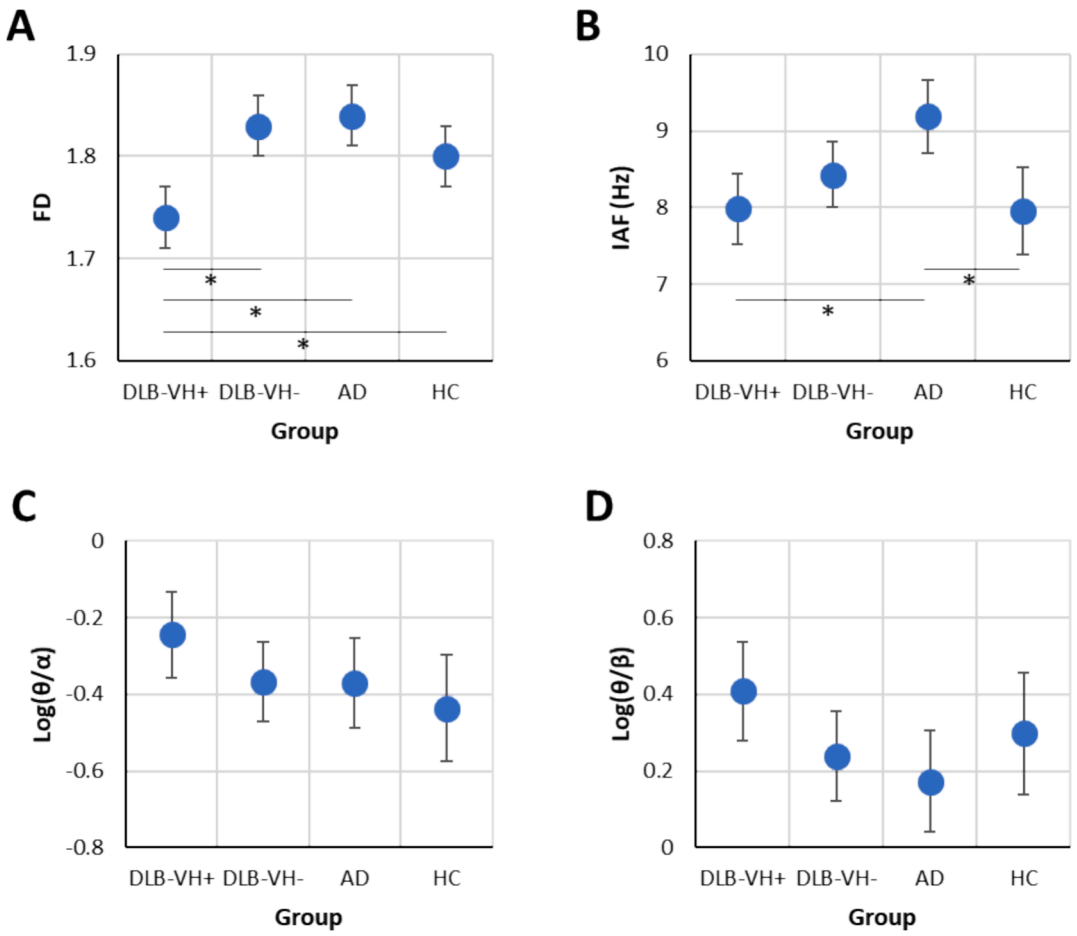

Fig. 1. Estimated Marginal Means from ANCOVA1. The figure shows marginal means of Higuchi's Fractal Dimension – FD (A), Individual Alpha Frequency – IAF (B), Log-transformed Theta/Alpha ratio – Log(θ/α) (C), and Theta/Beta ratio – Log(θ/β) (D) for the four groups: Dementia with Lewy bodies (DLB) patients with visual hallucinations (DLB-VH+), DLB patients without hallucinations (DLB-VH-), Alzheimer's disease patients (AD) and healthy controls (HC). Marginal means were estimated while accounting for MMSE and Age effects using ANCOVA1. Error bars indicate 95 % confidence intervals.

3.2. Entropy (En)

The results of the ANCOVA1 on En rs-EEG measures, which included MMSE scores and age as covariates, showed significant effects for Group ($F(3,128) = 5.893$, $p < 0.001$) but not for MMSE ($F(1,128) = 1.322$, $p = 0.252$) and Age ($F(1,128) = 0.905$, $p = 0.343$). En was significantly lower for DLB-VH+ compared to HC (DLB-VH+ vs. HC: $t(128) = -4.157$, $p < 001$), between DLB-VH- vs. HC: $t(128) = -3.052$, $p = 0.014$ and between AD vs HC: $t(128): -2.2559$, $p = 0.047$. No other comparison was significantly different. The results were almost identical to those obtained with ANCOVA2 and consistent with the ANOVA.

3.3. Individual alpha frequency (IAF)

The results of the ANCOVA1 on IAF measures (Fig. 1B) showed significant effects for Group ($F(3,128) = 5.592$, $p < 0.001$) and MMSE ($F(1,128) = 58.184$, $p < 0.001$), but not for Age ($F(1,128) = 0.014$, $p = 0.905$). Post-hoc tests revealed that IAF differed significantly between AD and DLB-VH+ ($t(128) = 3.708$, $p = 0.002$), AD and HC ($t(128) = 3.116$, $p = 0.011$), and a similar trend, although non-significant, was observed between AD and DLB-VH- ($t(128) = 2.345$, $p = 0.082$). All the other comparisons were not significantly different (all ps > 0.488). The results were almost identical to those obtained with ANCOVA2 (Figure S1B). In contrast, the ANOVA revealed a different pattern of results (Figure S2B). The post-hoc tests revealed significant differences only between the DLB-VH+ and the other groups (all ps < 0.005), while all the other contrasts were not significant (all ps > 0.917).

3.4. θ/α and θ/β ratios

The results of the ANCOVA1 on θ/α (Fig. 1C) revealed a significant effect for MMSE ($F(1,128) = 22.930$, $p < 0.001$), but not for Group ($F(3,128) = 1.579$, $p = 0.198$) or Age ($F(1,128) = 0.200$, $p = 0.656$). Very similar results were obtained from ANCOVA2 (Figure S1C). In contrast, the ANOVA revealed a significant Group effect ($F(3,130) = 8.68$, $p < 0.001$). Figure S2C shows that HC θ/α was significantly lower compared to DLB-VH+ ($t(130) = -4.99$, $p < 0.001$) and AD ($t(130) = -3.30$, $p = 0.006$). Moreover, θ/α was significantly higher for DLB-VH+ than DLB-VH- ($t(130) = 2.89$, $p = 0.018$).

The results of the ANCOVA1 on θ/β (Fig. 1D) revealed a significant effect for MMSE ($F(1,128) = 37.92$, $p < 0.001$), but not for Group ($F(3,128) = 2.46$, $p = 0.066$) or Age ($F(1,128) = 0.08$, $p = 0.780$). In ANCOVA2 (Figure S1D), the effect of Group reached the significance ($F(3,129) = 2.77$, $p = 0.044$), with a significantly higher θ/β for DLB-VH+ compared to AD ($t(128) = 0.243$, $p = 0.040$). No other contrasts were significant (all ps > 0.271). The ANOVA revealed a significant effect of group ($F(3,130) = 7.79$, $p < 0.001$). Similar to what observed in the other ANOVAs, Figure S2D shows that θ/β was significantly higher for DLB-VH+ compared to DLB-VH- ($t(128) = 3.544$, $p = 0.003$), AD ($t(128) = 2.830$, $p = 0.022$), and HC ($t(128) = 4.553$, $p < 0.001$).

4. Discussion

The primary result of this study was the discrimination between DLB patients presenting visual hallucinations (DLB-VH+) and all other

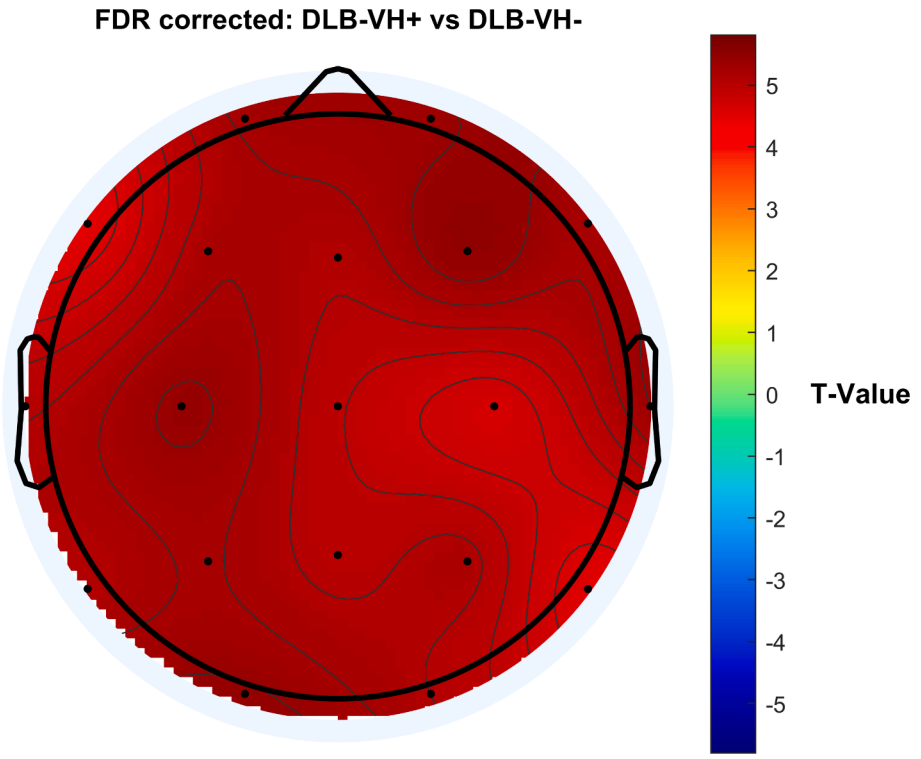

Fig. 2. Topographical representation of the non-parametric *t*-test between DLB-VH+ vs. DLB-VH- contrasts for FD. The results are FDR-corrected. The color bar represents the T-value of the non-parametric *t*-test.

groups based on the Higuchi's Fractal Dimension (FD) index. In particular, the FD index was found to be lower in DLB patients with visual hallucinations (DLB-VH+) compared to all other groups, including DLB-VH-. The latter finding, which was not replicated using another measure of complexity and uncertainty such as Entropy, was consistent across different analyses, including when controlling for the significant effect of global cognitive status (MMSE scores) and age. It is remarkable that this was the sole index that distinctly differentiated the DLB-VH+ group from all other groups, even after accounting for group differences in global cognitive status. Additionally, age did not significantly modulate the observed FD differences. This result suggests that the presence of visual hallucinations as a symptom in DLB is associated with an overall neuronal activity profile (measured with resting-state EEG) characterized by simpler dynamics, regardless of the cognitive severity and age.

The presence of visual hallucinations has been interpreted as due to disturbances not only in posterior brain regions linked to vision, but also to large-scale, distributed, function-critical neural networks (Ffytche, 2008; Shine et al., 2011). It is reasonable to assume that the degeneration and dysfunction of these extensive neural networks lead to a loss of global brain complexity, which is well captured by the FD index.

Differential complexity of EEG signal, as measured with the Higuchi's FD, has been observed when comparing a range of neuropsychiatric conditions such as ADHD (Mohammadi et al., 2016), schizophrenia (e.g., Raghavendra et al., 2009) and major depression (Bachmann et al., 2018; Cukic et al., 2020), where the typical result is an increased FD in these patients. On the contrary, in AD patients a lower FD with respect to controls is a typical finding (Nobukawa et al., 2019; Al-Nuaimi, Jammeh, Sun, Ifeachor, 2017; Smits et al., 2016).

In our study, we could not replicate the latter finding, as AD patients did not significantly differ from healthy controls in terms of FD. This could be partially explained by the fact that in our study, AD patients had, on average, higher MMSE scores (21.97 ± 5.34) than those included in previous works (Nobukawa et al., 2019: 15.5 ± 5.3; Smits et al., 2016: 20.6 ± 4.25; Al-Nuaimi et al., 2017). However, previous studies did not account for MMSE scores in their analyses. This could be problematic, as our data reveal that MMSE scores correlate across all dementia patient groups with both linear and non-linear electrophysiological indices. This highlights the importance of considering MMSE scores as a significant confounding factor in such works. Notwithstanding partial discrepancies with previous literature regarding the comparison between AD and controls, this study broadens this body of literature by reaffirming the discriminatory potential of this index within the domain of neurodegenerative disorders. This index, in particular, demonstrates a unique capability to differentiate DLB patients with VH not only from healthy controls but also from a sub-group of DLB patients without VH and AD, where differential diagnosis is often challenging.

Another noteworthy index is the IAF. Specifically, this index was higher in the Alzheimer's disease group than in the other groups (though only as a tendency for the DLB-VH-), but this difference was observed only when controlling for MMSE. If the global cognitive status was not taken into consideration, the pattern of results was completely different, with the IAF being lower in the DLB-VH+ group than all the other groups. Clearly, in this case, the IAF effect is heavily confounded with the severity of cognitive decline and could not be univocally interpreted in terms of its diagnostic power.

In contrast, the θ/α and θ/β indices covaried with MMSE scores, and could not distinguish across groups when the confounding effects of (significant) MMSE and (non-significant) age were taken into consideration. Interestingly, when MMSE effect was not controlled for, a lower θ/β characterized the DLB-VH+ group with respect to all the other groups, confirming previous literature showing that this index was associated with the presence of hallucinations in similar clinical populations (e.g., Baik et al., 2022).

Regarding the potential influence of psychoactive drugs on EEG findings in the DLB group, we argue that L-Dopa and benzodiazepines (clonazepam) could not have played any substantial role, the first being poorly represented in this study groups of VH+ vs VH-, the latter being equally distributed in the two DLB groups. The use of cholinesterase inhibitors would eventually have been in favor of an increased brain

activity in the VH + group, and in this case could have strengthened our conclusion. Finally, we cannot exclude that the use of atypical antipsychotic drugs in the VH+ group might have acted as a potential modulator of brain activity. However, the very low dosage of quetiapine used in chronic administration, the avoidance of long-lasting formulations, and the fact that its last intake occurred more than 12 h prior to the EEG recording, make the possibility of a substantial effect of this drug on our findings unlikely.

Among the strengths of our study, there is the fact that our sample of DLB patients had a long clinical follow-up encompassing a mean time of 6 years with confirmation of clinical diagnosis at each yearly visit. Moreover, Alzheimer's disease patients included did not suffer from hallucinations, which was an exclusion criterion for this group or other core features of DLB. Nonetheless, we acknowledge that the lack of biological diagnosis of AD in DLB patients or of pathological diagnosis is a limitation of this study.

Another strength of this study is that the computationally feasible Higuchi's FD measure, identified here as the most effective index for distinguishing hallucinating DLB patients from others, was applied to a brief standard 19-channel EEG recording without any a priori channel selection and any spectral transformation. These characteristics, including the non-transformed, low-density EEG data used in the analyses and the short recording time, strongly support the potential feasibility of employing this measure in routine clinical practice (Porcaro et al 2022b).

4.1. Limits and future Directions

While the sample sizes for the included groups were good for a monocenter study, replicating these findings in a multi-center study with larger sample sizes would be valuable. This replication could not only further corroborate the role of the FD index in discriminating between DLB-VH+ and other groups, but also shed light on whether some of the discrepancies with respect to the previous literature (primarily, Alzheimer's disease patients not showing lower FD than controls) were accountable for by the variability typical of relatively small sample sizes. In addition, although DLB and AD groups were strictly adherent to clinical diagnostic criteria and the diagnosis was confirmed during a long follow-up, we acknowledge that the lack of biological diagnosis of AD in DLB patients or of pathological diagnosis is a limitation of this study.

It is known that dominant slower EEG activity is present not only in DLB patients with visual hallucinations but also in Alzheimer's disease patients who experience visual hallucinations, compared to those without hallucinations (Dauwan, Linszen et al., 2018). While not including Alzheimer's disease patients with visual hallucinations helped obtaining a cleaner sample, it would be useful to also include a group of Alzheimer's disease patients with visual hallucinations in future studies, to check the discriminative capacity of the Higuchi's FD analysis when comparing different categories of clinical populations all presenting hallucinations as a common symptom, thus helping exploring a more transdiagnostic approach.

Lastly, it is important to note that the EEG data in this study were recorded using only 19 channels. This limitation hindered the possibility of conducting a more comprehensive analysis of the neurophysiological data, such as source analysis or fine-grained functional connectivity. It is however worth highlighting that this is a standard clinical practice montage, due to resource and time constraints. Despite the limitation represented by the low-density EEG dataset, the sensitivity of FD as a diagnostic tool in discriminating between DLB patients with visual hallucinations and other dementia patients and matched healthy controls, underscores the scalability of this analytical approach for routine clinical practice.

5. Conclusions

The key finding of this study was the identification of a resting-state EEG profile characterized by simpler dynamics in DLB patients presenting visual hallucinations (DLB-VH+) compared to all other groups. This distinction, revealed through Higuchi's FD index, persisted even after accounting for variability related to the global cognitive status. In this regard, this nonlinear index surpassed other more traditional linear and non-linear measures considered, including individual alpha frequency, the ratio between theta and higher frequencies, and entropy, in terms of discriminability between hallucinating DLB patients and all other patients, including a non-hallucinating DLB sub-group.

In summary, the sensitivity and scalability of FD suggest that this non-linear index of EEG dynamics is not only crucial for elucidating the neural underpinnings of pervasive symptoms like visual hallucinations in DLB, but also holds potential for seamless integration into established clinical workflows tailored to various DLB subtypes. Future research ought to determine whether FD could serve as a valuable tool not only for improving diagnostic precision, but also for evaluating the effectiveness of diverse interventions, and ultimately refining prognostic assessments.

CRediT authorship contribution statement

Vallesi Antonino: Conceptualization, Project administration, Methodology, Writing – original draft, Writing – review & editing. **Porcaro Camillo:** Methodology, Data curation, Formal analysis, Writing – review & editing, Visualization. **Visalli Antonino:** Methodology, Data curation, Formal analysis, Writing – review & editing, Visualization. **Fasolato Davide:** Writing – review & editing. **Rossato Francesco:** Writing – review & editing. **Bussè Cinzia:** Writing – review & editing. **Cagnin Annachiara:** Conceptualization, Project administration, Resources, Data curation, Writing – review & editing.

Declaration of Competing Interest

The authors declare that they have no known competing financial interests or personal relationships that could have appeared to influence the work reported in this paper.

Acknowledgments

This research was partially supported by funding from the "Progetto Giovani Ricercatori: FINAGE (GR- 2018- 12367927) to AVal from the Italian Ministry of Health.

Appendix A. Supplementary data

Supplementary data to this article can be found online at https://doi.org/10.1016/j.clinph.2024.10.004.

References

Aarsland, D., Ballard, C., Larsen, J.P., McKeith, I., 2001. A comparative study of psychiatric symptoms in dementia with Lewy bodies and Parkinson's disease with and without dementia. Int. J. Geriatr. Psychiatry 16, 528–536. https://doi.org/10.1002/gps.389.

Al-Nuaimi, A.H., Jammeh, E., Sun, L., Ifeachor, E., 2017. Higuchi fractal dimension of the electroencephalogram as a biomarker for early detection of Alzheimer's disease. Annu. Int. Conf. IEEE Eng. Med. Biol. Soc. 2017, 2320–2324. https://doi.org/10.1109/EMBC.2017.8037320.

Aoki, Y., Kazui, H., Pascal-Marqui, R.D., Ishii, R., Yoshiyama, K., Kanemoto, H., Suzuki, Y., Sato, S., Hata, M., Canuet, L., Iwase, M., Ikeda, M., 2019. EEG resting-state networks in dementia with lewy bodies associated with clinical symptoms. Neuropsychobiology 77, 206–218. https://doi.org/10.1159/000495620.

Bachmann, M., Päeske, L., Kalev, K., Aarma, K., Lehtmets, A., Ööpik, P., Lass, J., Hinrikus, H., 2018. Methods for classifying depression in single channel EEG using linear and nonlinear signal analysis. Comput. Methods Programs Biomed. 155, 11–17. https://doi.org/10.1016/j.cmpb.2017.11.023.

Baik, K., Jung, J.H., Jeong, S.H., Chung, S.J., Yoo, H.S., Lee, P.H., Sohn, Y.H., Kang, S.W., Ye, B.S., 2022. Implication of EEG theta/alpha and theta/beta ratio in Alzheimer's and Lewy body disease. Sci. Rep. 12, 18706. https://doi.org/10.1038/s41598-022-21951-5.

Barbati, G., Porcaro, C., Zappasodi, F., Rossini, P.M., Tecchio, F., 2004. Optimization of an independent component analysis approach for artifact identification and removal in magnetoencephalographic signals. Clin. Neurophysiol. 115 (5), 1220–1232. https://doi.org/10.1016/j.clinph.2003.12.015.

Bonanni, L., Thomas, A., Tiraboschi, P., Perfetti, B., Varanese, S., Onofrj, M., 2008. EEG comparisons in early Alzheimer's disease, dementia with Lewy bodies and Parkinson's disease with dementia patients with a 2-year follow-up. Brain 131, 690–705. https://doi.org/10.1093/brain/awm322.

Bonanni, L., Franciotti, R., Nobili, F., Kramberger, M.G., Taylor, J.-P., Garcia-Ptacek, S., Falasca, N.W., Famá, F., Cromarty, R., Onofrj, M., Aarsland, D., E-DLB study group, 2016. EEG markers of dementia with lewy bodies: a multicenter cohort study. J. Alzheimers Dis. 54, 1649–1657. https://doi.org/10.3233/JAD-160435.

Chatzikonstantinou, S., McKenna, J., Karantali, E., Petridis, F., Kazis, D., Mavroudis, I., 2021. Electroencephalogram in dementia with Lewy bodies: a systematic review. Aging Clin. Exp. Res. 33, 1197–1208. https://doi.org/10.1007/s40520-020-01576-2.

Cohen, M.X., 2015. Comparison of different spatial transformations applied to EEG data: A case study of error processing. Int. J. Psychophysiol. 97 (3), 245–257. https://doi.org/10.1016/j.ijpsycho.2014.09.013.

Cole, S.R., Voytek, B., 2017. Brain oscillations and the importance of waveform shape. Trends Cogn. Sci. 21 (2), 137–149. https://doi.org/10.1016/j.tics.2016.12.008.

Collerton, D., Burn, D., McKeith, I., O'Brien, J., 2003. Systematic review and meta-analysis show that dementia with Lewy bodies is a visual-perceptual and attentional-executive dementia. Dement. Geriatr. Cogn. Disord. 16, 229–237. https://doi.org/10.1159/000072807.

Corcoran, A.W., Alday, P.M., Schlesewsky, M., Bornkessel-Schlesewsky, I., 2018. Toward a reliable, automated method of individual alpha frequency (IAF) quantification. Psychophysiology 55 (7), e13064.

Cottone, C., Porcaro, C., Cancelli, A., Olejarczyk, E., Salustri, C., Tecchio, F., 2017. Neuronal electrical ongoing activity as a signature of cortical areas. Brain Struct. Funct. 222, 2115–2126. https://doi.org/10.1007/s00429-016-1328-4.

Cukic, M., Stokic, M., Radenkovic, S., Ljubisavljevic, M., Simic, S., Savic, D., 2020. Nonlinear analysis of EEG complexity in episode and remission phase of recurrent depression. Int. J. Methods Psychiatr. Res. 29 (2), e1816.

Cummings, J.L., 1997. The Neuropsychiatric Inventory: assessing psychopathology in dementia patients. Neurology 48, S10–S16. https://doi.org/10.1212/wnl.48.5_suppl_6.10s.

D'Antonio, F., Boccia, M., Di Vita, A., Suppa, A., Fabbrini, A., Canevelli, M., Caramia, F., Fiorelli, M., Guariglia, C., Ferracuti, S., de Lena, C., Aarsland, D., Ffytche, D., 2022. Visual hallucinations in Lewy body disease: pathophysiological insights from phenomenology. J. Neurol. 269, 3636–3652. https://doi.org/10.1007/s00415-022-10983-6.

Dauwan, M., Linszen, M.M.J., Lemstra, A.W., Scheltens, P., Stam, C.J., Sommer, I.E., 2018. EEG-based neurophysiological indicators of hallucinations in Alzheimer's disease: Comparison with dementia with Lewy bodies. Neurobiol. Aging 67, 75–83. https://doi.org/10.1016/j.neurobiolaging.2018.03.013.

Dauwan, M., Hoff, J.I., Vriens, E.M., Hillebrand, A., Stam, C.J., Sommer, I.E., 2019. Aberrant resting-state oscillatory brain activity in Parkinson's disease patients with visual hallucinations: An MEG source-space study. Neuroimage Clin 22, 101752. https://doi.org/10.1016/j.nicl.2019.101752.

Delorme, A., Makeig, S., 2004. EEGLAB: an open source toolbox for analysis of single-trial EEG dynamics including independent component analysis. J. Neurosci. Methods 134, 9–21. https://doi.org/10.1016/j.jneumeth.2003.10.009.

Diederich, N.J., Goetz, C.G., Stebbins, G.T., 2005. Repeated visual hallucinations in Parkinson's disease as disturbed external/internal perceptions: focused review and a new integrative model. Mov. Disord. 20, 130–140. https://doi.org/10.1002/mds.20308.

Donaghy, P.C., Carrarini, C., Ferreira, D., Habich, A., Aarsland, D., Babiloni, C., Bayram, E., Kane, J.P., Lewis, S.J., Pilotto, A., Thomas, A.J., Bonanni, L., 2023. Alzheimer's Association International Society to Advance Alzheimer's Research and Treatment Lewy Body Dementias Prodromal Working Group. Research diagnostic criteria for mild cognitive impairment with Lewy bodies: A systematic review and meta-analysis. Alzheimers Dement. 19 (7), 3186–3202. https://doi.org/10.1002/alz.13105.

Esteller, R., Vachtsevanos, G., Echauz, J., Litt, B., 2001. A comparison of waveform fractal dimension algorithms. I.E.E.E. Trans. Biomed. Eng. 48 (2), 177–183. https://doi.org/10.1109/81.904882.

Ffytche, D.H., 2008. The hodology of hallucinations. Cortex 44, 1067–1083. https://doi.org/10.1016/j.cortex.2008.04.005.

Fiorenzato, E., Moaveninejad, S., Weis, L., Biundo, R., Antonini, A., Porcaro, C., 2023. Brain dynamics complexity as a signature of cognitive decline in parkinson's disease. Mov. Disord. https://doi.org/10.1002/mds.29678.

Folstein, M.F., Folstein, S.E., McHugh, P.R., 1975. "Mini-mental state". A practical method for grading the cognitive state of patients for the clinician. J. Psychiatr. Res. 12 (3), 189–198. https://doi.org/10.1016/0022-3956(75)90026-6.

Freedman, D., Diaconis, P., 1981. On the histogram as a density estimator: L2 theory". Probab. Theory Relat. Fields 57 (4), 453–476.

Harding, A.J., Broe, G.A., Halliday, G.M., 2002. Visual hallucinations in Lewy body disease relate to Lewy bodies in the temporal lobe. Brain 125, 391–403. https://doi.org/10.1093/brain/awf033.

Heitz, C., Noblet, V., Cretin, B., Philippi, N., Kremer, L., Stackfleth, M., Hubele, F., Armspach, J.P., Namer, I., Blanc, F., 2015. Neural correlates of visual hallucinations in dementia with Lewy bodies. Alzheimers Res. Ther. 7, 6. https://doi.org/10.1186/s13195-014-0091-0.

Higuchi, T., 1988. Approach to an irregular time series on the basis of the fractal theory. Phys. D Nonlinear Phenom. 31, 277–283. https://doi.org/10.1016/0167-2789(88)90081-4.

Holroyd, S., Currie, L., Wooten, G.F., 2001. Prospective study of hallucinations and delusions in Parkinson's disease. J. Neurol. Neurosurg. Psychiatry 70, 734–738. https://doi.org/10.1136/jnnp.70.6.734.

Hyvärinen, A., Oja, E., 2000. Independent component analysis: algorithms and applications. Neural Netw. 13, 411–430. https://doi.org/10.1016/s0893-6080(00)00026-5.

Ibarretxe-Bilbao, N., Ramirez-Ruiz, B., Junque, C., Marti, M.J., Valldeoriola, F., Bargallo, N., Juanes, S., Tolosa, E., 2010. Differential progression of brain atrophy in Parkinson's disease with and without visual hallucinations. J. Neurol. Neurosurg. Psychiatry 81, 650–657. https://doi.org/10.1136/jnnp.2009.179655.

IFSECN, 1974. A glossary of terms most commonly used by clinical electroencephalographers. Electroencephalogr. Clin. Neurophysiol. https://doi.org/10.1016/0013-4694(74)90099-6.

Jicha, G.A., Schmitt, F.A., Abner, E., Nelson, P.T., Cooper, G.E., Smith, C.D., Markesbery, W.R., 2010. Prodromal clinical manifestations of neuropathologically confirmed Lewy body disease. Neurobiol. Aging 31, 1805–1813. https://doi.org/10.1016/j.neurobiolaging.2008.09.017.

Jones, S.R., 2016. When brain rhythms aren't 'rhythmic': implication for their mechanisms and meaning. Curr. Opin. Neurobiol. 40, 72–80. https://doi.org/10.1016/j.conb.2016.06.010.

Law, Z.K., Todd, C., Mehraram, R., Schumacher, J., Baker, M.R., LeBeau, F.E.N., Yarnall, A., Onofrj, M., Bonanni, L., Thomas, A., Taylor, J.-P., 2020. The Role of EEG in the Diagnosis, Prognosis and Clinical Correlations of Dementia with Lewy Bodies-A Systematic Review. Diagnostics (Basel) 10, 616. https://doi.org/10.3390/diagnostics10090616.

Marino, M., Liu, Q., Samogin, J., Tecchio, F., Cottone, C., Mantini, D., Porcaro, C., 2019. Neuronal dynamics enable the functional differentiation of resting state networks in the human brain. Hum. Brain Mapp. 40, 1445–1457. https://doi.org/10.1002/hbm.24458.

McKeith, I.G., Boeve, B.F., Dickson, D.W., Halliday, G., Taylor, J.-P., Weintraub, D., Aarsland, D., Galvin, J., Attems, J., Ballard, C.G., Bayston, A., Beach, T.G., Blanc, F., Bohnen, N., Bonanni, L., Bras, J., Brundin, P., Burn, D., Chen-Plotkin, A., Duda, J.E., El-Agnaf, O., Feldman, H., Ferman, T.J., Ffytche, D., Fujishiro, H., Galasko, D., Goldman, J.G., Gomperts, S.N., Graff-Radford, N.R., Honig, L.S., Iranzo, A., Kantarci, K., Kaufer, D., Kukull, W., Lee, V.M.Y., Leverenz, J.B., Lewis, S., Lippa, C., Lunde, A., Masellis, M., Masliah, E., McLean, P., Mollenhauer, B., Montine, T.J., Moreno, E., Mori, E., Murray, M., O'Brien, J.T., Orimo, S., Postuma, R.B., Ramaswamy, S., Ross, O.A., Salmon, D.P., Singleton, A., Taylor, A., Thomas, A., Tiraboschi, P., Toledo, J.B., Trojanowski, J.Q., Tsuang, D., Walker, Z., Yamada, M., Kosaka, K., 2017. Diagnosis and management of dementia with Lewy bodies: Fourth consensus report of the DLB Consortium. Neurology 89, 88–100. https://doi.org/10.1212/WNL.0000000000004058.

McKhann, G.M., Knopman, D.S., Chertkow, H., Hyman, B.T., Jack, C.R., Kawas, C.H., Klunk, W.E., Koroshetz, W.J., Manly, J.J., Mayeux, R., Mohs, R.C., Morris, J.C., Rossor, M.N., Scheltens, P., Carrillo, M.C., Thies, B., Weintraub, S., Phelps, C.H., 2011. The diagnosis of dementia due to Alzheimer's disease: recommendations from the National Institute on Aging-Alzheimer's Association workgroups on diagnostic guidelines for Alzheimer's disease. Alzheimers Dement. 7, 263–269. https://doi.org/10.1016/j.jalz.2011.03.005.

Mehraram, R., Peraza, L.R., Murphy, N.R.E., Cromarty, R.A., Graziadio, S., O'Brien, J.T., Killen, A., Colloby, S.J., Firbank, M., Su, L., Collerton, D., Taylor, J.P., Kaiser, M., 2022. Functional and structural brain network correlates of visual hallucinations in Lewy body dementia. Brain 145, 2190–2205. https://doi.org/10.1093/brain/awac094.

Merdes, A.R., Hansen, L.A., Jeste, D.V., Galasko, D., Hofstetter, C.R., Ho, G.J., Thal, L.J., Corey-Bloom, J., 2003. Influence of Alzheimer pathology on clinical diagnostic accuracy in dementia with Lewy bodies. Neurology 60, 1586–1590. https://doi.org/10.1212/01.wnl.0000065889.42856.f2.

Moaveninejad, S., D'Onofrio, V., Tecchio, F., Ferracuti, F., Iarlori, S., Monteriù, A., Porcaro, C., 2024. Fractal Dimension as a discriminative feature for high accuracy classification in motor imagery EEG-based brain-computer interface. Comput. Methods Programs Biomed. 244, 107944. https://doi.org/10.1016/j.cmpb.2023.107944.

Mohammadi, M.R., Khaleghi, A., Nasrabadi, A.M., Rafieivand, S., Begol, M., Zarafshan, H., 2016. EEG classification of ADHD and normal children using non-linear features and neural network. Biomed. Eng. Lett. 6 (2), 66–73.

Nelson, P.T., Jicha, G.A., Kryscio, R.J., Abner, E.L., Schmitt, F.A., Cooper, G., Xu, L.O., Smith, C.D., Markesbery, W.R., 2010. Low sensitivity in clinical diagnoses of dementia with Lewy bodies. J. Neurol. 257, 359–366. https://doi.org/10.1007/s00415-009-5324-y.

Nobukawa, S., Yamanishi, T., Nishimura, H., Wada, Y., Kikuchi, M., Takahashi, T., 2019. Atypical temporal-scale-specific fractal changes in Alzheimer's disease EEG and their relevance to cognitive decline. Cogn. Neurodyn. 13 (1), 1–11.

Onofrj, M., Espay, A.J., Bonanni, L., Delli Pizzi, S., Sensi, S.L., 2019. Hallucinations, somatic-functional disorders of PD-DLB as expressions of thalamic dysfunction. Mov. Disord. 34, 1100–1111. https://doi.org/10.1002/mds.27781.

Oppedal, K., Borda, M.G., Ferreira, D., Westman, E., Aarsland, D., 2019. European DLB consortium: diagnostic and prognostic biomarkers in dementia with Lewy bodies, a multicenter international initiative. Neurodegenerative Disease Management 9, 247–250. https://doi.org/10.2217/nmt-2019-0016.

Peraza, L.R., Cromarty, R., Kobeleva, X., Firbank, M.J., Killen, A., Graziadio, S., Thomas, A.J., O'Brien, J.T., Taylor, J.-P., 2018. Electroencephalographic derived network differences in Lewy body dementia compared to Alzheimer's disease patients. Sci. Rep. 8, 4637. https://doi.org/10.1038/s41598-018-22984-5.

Perry, E.K., Marshall, E., Kerwin, J., Smith, C.J., Jabeen, S., Cheng, A.V., Perry, R.H., 1990. Evidence of a monoaminergic-cholinergic imbalance related to visual hallucinations in Lewy body dementia. J. Neurochem. 55, 1454–1456. https://doi.org/10.1111/j.1471-4159.1990.tb03162.x.

Perry, E., Walker, M., Grace, J., Perry, R., 1999. Acetylcholine in mind: a neurotransmitter correlate of consciousness? Trends Neurosci. 22, 273–280. https://doi.org/10.1016/s0166-2236(98)01361-7.

Pion-Tonachini, L., Kreutz-Delgado, K., Makeig, S., 2019. ICLabel: An automated electroencephalographic independent component classifier, dataset, and website. Neuroimage 198, 181–197. https://doi.org/10.1016/j.neuroimage.2019.05.026.

Porcaro, C., Medaglia, M.T., Krott, A., 2015. Removing speech artifacts from electroencephalographic recordings during overt picture naming. Neuroimage 105, 171–180.

Porcaro, C., Cottone, C., Cancelli, A., Rossini, P.M., Zito, G., Tecchio, F., 2019. Cortical neurodynamics changes mediate the efficacy of a personalized neuromodulation against multiple sclerosis fatigue. Sci. Rep. 9 (1), 18213. https://doi.org/10.1038/s41598-019-54595-z.

Porcaro, C., Mayhew, S.D., Marino, M., Mantini, D., Bagshaw, A.P., 2020. Characterisation of haemodynamic activity in resting state networks by fractal analysis. S0129065720500616 Int. J. Neural Syst. 30. https://doi.org/10.1142/S0129065720500616.

Porcaro, C., Vecchio, F., Miraglia, F., Zito, G., Rossini, P.M., 2022b. Dynamics of the "Cognitive" brain wave P3b at rest for alzheimer dementia prediction in mild cognitive impairment. Int. J. Neural Syst. 32 (5), 2250022. https://doi.org/10.1142/S0129065722500228.

Porcaro, C., Moaveninejad, S., D'Onofrio, V., DiIeva, A., 2024. Fractal time series: background, estimation methods, and performances. Adv. Neurobiol. 36, 95–137. https://doi.org/10.1007/978-3-031-47606-8_5.

Raghavendra, B., Dutt, D.N., Halahalli, H.N., John, J.P., 2009. Complexity analysis of EEG in patients with schizophrenia using fractal dimension. Physiol. Meas. 30 (8), 795.

Ramon, C., Holmes, M.D., 2015. Spatiotemporal phase clusters and phase synchronization patterns derived from high density EEG and ECoG recordings. Curr. Opin. Neurobiol. 31, 127–132. https://doi.org/10.1016/j.conb.2014.10.001.

Roks, G., Korf, E.S.C., van der Flier, W.M., Scheltens, P., Stam, C.J., 2008. The use of EEG in the diagnosis of dementia with Lewy bodies. J. Neurol. Neurosurg. Psychiatry 79, 377–380. https://doi.org/10.1136/jnnp.2007.125385.

Rubega, M., Scarpa, F., Teodori, D., Sejling, A.-S., Frandsen, C.S., Sparacino, G., 2020. Detection of hypoglycemia using measures of EEG complexity in type 1 diabetes patients. Entropy 22 (1), 81. https://doi.org/10.3390/e22010081.

Shine, J.M., Halliday, G.M., Naismith, S.L., Lewis, S.J., 2011. Visual misperceptions and hallucinations in Parkinson's disease: dysfunction of attentional control networks? Mov. Disord. 26 (12), 2154–2159. https://doi.org/10.1002/mds.23896.

Smits, F.M., Porcaro, C., Cottone, C., Cancelli, A., Rossini, P.M., Tecchio, F., 2016. Electroencephalographic fractal dimension in healthy ageing and Alzheimer's disease. PLoS One 11, e0149587.

Tiraboschi, P., Hansen, L.A., Alford, M., Sabbagh, M.N., Schoos, B., Masliah, E., Thal, L. J., Corey-Bloom, J., 2000. Cholinergic dysfunction in diseases with Lewy bodies. Neurology 54, 407–411. https://doi.org/10.1212/wnl.54.2.407.

Tiraboschi, P., Salmon, D.P., Hansen, L.A., Hofstetter, R.C., Thal, L.J., Corey-Bloom, J., 2006. What best differentiates Lewy body from Alzheimer's disease in early-stage dementia? Brain 129, 729–735. https://doi.org/10.1093/brain/awh725.

Yoshizawa, H., Vonsattel, J.P.G., Honig, L.S., 2013. Presenting neuropsychological testing profile of autopsy-confirmed frontotemporal lobar degeneration. Dement. Geriatr. Cogn. Disord. 36, 279–289. https://doi.org/10.1159/000353860.

Zorzi, G., Thiebaut de Schotten, M., Manara, R., Bussè, C., Corbetta, M., Cagnin, A., 2021. White matter abnormalities of right hemisphere attention networks contribute to visual hallucinations in dementia with Lewy bodies. Cortex 139, 86–98. https://doi.org/10.1016/j.cortex.2021.03.007.